Brazilian Journal
of Chemical
Engineering

ISSN 0104-6632
Printed in Brazil
www.abeq.org.br/bjche

Vol. 36, No. 04, pp. 1571 - 1586, October - December, 2019
dx.doi.org/10.1590/0104-6632.20190364s20190270

PREPARATION AND SIMULATION OF THE ON-LINE SiO_2/S COATING FOR COKING INHIBITION IN THE INDUSTRIAL CRACKING FURNACE

Zhiyuan Wang[1*], Xudong Ding[1] and Guanping Huo[1]

[1] University of Shanghai for Science and Technology, School of Energy and Power Engineering, Shanghai Key Laboratory of Multiphase Flow and Heat Transfer in Power Engineering, Shanghai, China. E-mail: wzy_1983@163.com - ORCID: 0000-0002-5990-9193

(Submitted: June 1, 2019 ; Revised: August 12, 2019 ; Accepted: August 20, 2019)

Abstract - Coke formation inside radiant coils is one of the main problems during thermal cracking of hydrocarbons. The on-line preparation of the coating for coking inhibition is a promising technology because it provides more flexibility to the operators on site. The SiO_2/S coating was prepared on the inner surface of coils in an 8-year-served GK-VI industrial cracking furnace. The effects of the coating preparation process on the operation of TLE were studied. The coking rates of the tube with and without coating preparation were evaluated by the trend change of tube metal temperature. Simulations of the coating deposition process were further carried out using the computational fluid dynamics approach. The results showed that a significant temperature increase at the outlets of TLEs during coating preparation were due to the accumulation of SiO_2 and S in a loose form under the TLE operating conditions when the concentration of coating precursors was 7500 ppm (wt. %). In the three tests, coating precursors were mainly completely consumed in tubes and TLEs. For the coated tube, the run time was extended by 4-7 days because the catalytic coking was decreased. No significant changes in the distribution of products and molar yields of main products were observed. In the simulations, it was found that increasing the inlet flow rate led to a more uniform thickness and improved the mass content of sulfur in the coating. In the tube bend section, circumferential nonuniformities for the deposition were due to circumferential differences in the temperatures and mass fractions. The mass fraction of S in the coating was within the range of 0.02%-0.1%. The control step for the SiO_2/S coating deposition was kinetic. Based on the simulation results, the optimized coating preparation parameters were determined, i.e., the inlet flow rate of 15t/h, the outlet temperature of 1093K and the inlet mass concentration of 3000 ppm (wt. %).

Keywords: Industrial cracking furnace; On-line SiO_2/S coating; Coke formation; CFD; Coating deposition.

INTRODUCTION

Steam cracking of hydrocarbon is the main process for the production of many base chemicals such as light olefins and aromatics. Coke formation is one of the main problems in steam cracking that deposits inside the radiant coils and the tubes of TLEs. As coke accumulates, the pressure drop increases gradually over the coil, leading to a decrease in the productivity and ethylene selectivity. Moreover, the additional heat must be supplied continuously to maintain the same cracking selectivity because the coke layer acts as an extra resistance for the heat transfer to the cracking gas. Eventually either the higher tube metal temperature (TMT) or an excessive pressure drop forces the furnace to be taken out of service and decoke the reactors. Decoking is undesirable because the production has to be halted for about 48 h. Additionally, the deterioration of the tube material is more pronounced after several cracking/decoking cycles due to the repeated exposure at high operating temperatures.

* Corresponding author: Zhiyuan Wang - E-mail: wzy_1983@163.com

In general, three coke formation mechanisms have been delineated (Gandarillas et al., 2014; Reyniers et al., 1994): the heterogeneous catalytic mechanism, the heterogeneous free-radical mechanism and the homogeneous droplets condensation/tar deposition mechanism. In the catalytic mechanism, tube metal materials (such as Fe and Ni) catalyze the dehydrogenation of hydrocarbons at high temperatures, which induces the formation of filamentous coke with Ni or Fe particles at the growing tip. When the inner wall of the tube is exposed to hydrocarbons at the initial stage, the catalytic mechanism dominates and coke deposits are quickly formed. In the second mechanism, coke precursors from the gas-phase, including free radicals, olefins, aromatics, etc., react with the coke surface via radical reactions. In the third mechanism, coke formation comes from heavy polynuclear aromatics present in the feed or formed from secondary chemical condensation reactions, which condense either on the wall or in the bulk gas phase, and then accumulate on the tube wall.

A lot of effort has been made for the suppression of coke formation, including surface pretreatments (Bao et al., 2018), coatings (Tang et al., 2014; Schietekat et al., 2015) and the application of additives (Wang et al., 2008; Rahimi et al., 2014). Coating technology has been widely used in the past 30 years in steam cracking because of the low effects on the target product yields and the normal operation of a cracker, the low operational cost, though a continuous addition is needed when the additives are applied, and the good coking inhibition property. The on-line preparation of a coating is a promising technique, which offers the advantages that the pretreatment process with some kinds of additives can be carried out at the heating stage of a cracking furnace after the decoking operation. Compared to the off-line coating technology, the on-line coating provide more flexibility to the operators on site. For example, no specialized device for the coating preparation is required and the inner surface of a cracking tube can be coated repeatedly to repair the coating.

Silicon-containing and related compounds are commonly used for coking inhibition in steam cracking. The application methods of using these compounds include pretreatment of the inner surface of the cracking coils, continuous addition of the additives during cracking, and the combination of pretreatment followed by continuous addition (Wang et al., 2008). However, the industrial application of these methods is difficult. The reason, at least partly, is that scaling up the methods based on results in laboratory-scale reactors is limited by many industrial factors. Laboratory scale studies do not necessarily reflect the operating conditions in industrial furnaces. For example, as low Reynolds numbers are employed in most lab-scale reactors, the physical impact of coking precursors moving to the inner surfaces to promote coke formation may be underestimated in lab-scale studies. Subsequently, the application methods present very excellent anti-coking effects when they are evaluated on the lab scale. Other factors, such as the metal surface conditions, the structural form of a cracker, the effects of the application methods on the downstream process, etc., also matter greatly when an industrial scale is considered. Each of those factors may limit the scope and applicability of the methods.

Some investigations concerning the effects of the on-line coatings containing Si on the coke formation during steam cracking have been carried out in laboratory-scale and pilot-scale reactors (Wang et al., 2007; Wang et al., 2008; Woerde et al., 2002; Zhou et al., 2007; Zhou et al., 2011). The anti-coking SiO_2/S coating has been prepared in a pilot-scale reactor in our earlier work using the mixture of tetraethylorthosilicate (TEOS) and dimethyldisulfide (DMDS) as source materials, which reduced coke yield by 40% in a 66h cracking run under naphtha cracking conditions (Zhou et al., 2011). The SiO_2/S coating includes silica and sulfur, possessing Si-O-S, O-Si-O and Si-O-Si structures. To apply the on-line coating technology in an industrial furnace, there are still some aspects that should be considered, as mentioned above. In this paper, the on-line coating technology was applied in an industrial cracker and the anti-coking properties of the SiO_2/S coating were evaluated. Specially, related industrial factors, such as the effects of the coating preparation process on TLEs, the metal surface conditions and other similar influences were investigated and discussed. The coating deposition is further investigated by using the computational fluid dynamics (CFD) approach in order to obtain reasonable operational conditions for coating preparation. The effects of inlet flow rate on the coating deposition rate, the mass fractions of intermediates and the control step of the deposition process are studied. Up to now few reports about the application of the on-line coating in an industrial scale cracking furnace have been published. The experimental results will be valuable for the further application of the on-line coating method, especially for the application methods involving silicon-containing compounds.

EXPERIMENTAL

Test furnace

The preparation of the SiO_2/S coating was performed in an 8-year-served GK-VI industrial cracking furnace, which includes the radiant section, the crossover section, the convection section and the quenching section. 48 reactor coils of the U type with 2 passes each are suspended side by side in the center of the furnace. The first pass of the coil is made of

Cr25Ni35 alloy with an inner diameter of 36 mm, while it is Cr35Ni45 alloy with an inner diameter of 48 mm for the second pass. Three TLEs positioned on top of the firebox are for quenching the cracking gas from the outlets of coils. The TLE consists of a waste heat boiler that recovers heat from the cracking gas by the production of high pressure steam. The ethylene yield is greatly dependent on the cracking temperature and the residence time of the hydrocarbons in the reactor coil. The operating conditions of the GK-VI cracking furnace and TLEs are given in Table 1. In general, it is desirable for GK-VI industrial cracking furnace to obtain the maximum ethylene yield.

Table 1. Cracking furnace dimensions and operating conditions.

Parameters		
Furnace segment		
Length (m)	9750	
Width (m)	2670	
Height (m)	14110	
Number of side burners	108	
Number of wall burners	24	
Reactor coils		
Number of reactor tubes	48	
Number of passes	2	
Inlet tube diameter(10^{-3} m)	36	
Outlet tube diameter(10^{-3} m)	48	
Steam dilution ratio (wt%)	0.7	
COT (K)	1110	
CIT (K)	873	
CIP (MPa)	0.21	
COP (Mpa)	0.10	
Naphtha (t/h)	26	
Fuel gas (t/h)	3.4	
Residence time (s)	0.23	
Feedstock composition (wt %)		
n-paraffins	42.886	
i-paraffins	34.111	
olefins	13.377	
aromatics	10.067	
Process parameters of TLE	**Shell side**	**Tube side**
Design pressure (MPa)	13.5	0.35
Working pressure (MPa)	12.08	0.106
Design temperature (inlet) (K)	370	900
Design temperature (center)(K)	350	450
Design temperature (outlet)(K)	340	525
Working temperature (inlet)(K)	325.5	829.8
Working temperature (outlet) (K)	326	378.1
Working medium	Water/steam	Cracking gas
Heat transfer area (m^2)	76.11	/
Steam yield (t/h)	130	/
Conditions of coating preparation		
TEOS + DMDS (L/h)	60	100	150
CIT(K)	873	873	873
COT(K)	1093	1103	1103
Steam (t/h)	20	20	20
Time (h)	4	3	4

Decoking operation

During the decoking in the radiant coils, the furnace is taken out of production to remove the coke layer by a controlled burning with a mixture of steam and air. At the beginning of this process, only steam is used. The coke is removed from the inner surface of the coil by the thermal shock, which causes the crushing of the coke layer. Then the crushed coke with a certain size is entrained by the effluent. Subsequently, steam is gradually reduced and the amount of air is increased. Diluted air mixture is used to avoid excessive tube skin temperatures because of the exothermic reaction between the coke layer and the mixture. CO_2 concentration in the effluent is determined by infrared analyzers every 30 minutes through the whole process. The decoking operation is regarded to be finished when the CO_2 concentration measured in the effluent is lower than 0.5%. After decoking the radiant coils, the furnace is cooled down to decoke the TLEs or to be repaired.

Coke is also formed in the tubes of the TLE, where both cracking and vapor cooling occurred. It is possible that all three mechanisms of coke formation were involved under TLE conditions. However, one of them may play a dominant role under a particular condition (Van Geem et al., 2009). Coke deposits on the wall of the TLE increase heat transfer resistances, which lead to a slow temperature increase at the outlet of the TLE. When the temperature exceeds the upper limit, the furnace needs to be shut down for decoking either mechanically or by passing a mixture of steam and air through the TLE to burn off the coke.

Coating preparation

The preparation of the on-line SiO_2/S coating was carried out after decoking the radiant coils and the TLEs. Dimethyldisulfide (DMDS) and tetraethylorthosilicate (TEOS) were mixed to pretreat the coils before the next production. The conditions of the coating preparation are given in Table 1. The coating precursors were introduced into the main steam pipeline using a syringe pump, where the coating precursors were mixed with steam at about 453 K.

Cracking process

After the coating preparation, the reactor coils were cooled down to 1023K in a steam flow. Then the naphtha feed was mixed with steam and the mixture gas was gradually raised to the normal cracking temperature. During the cracking process, the cracking gas was sampled every 15 days to analyze the effects of the coating on the yields of products by gas chromatography (Agilent 6890). The anti-coking property of the on-line coating was evaluated by analyzing the tube metal temperature (TMT) trends as a function of the run time. TMT was measured near the outlet of the tube by an infrared radiator (see Fig.1) at a fixed position of the furnace, and the profile of the first cracking run after every test was used to evaluate the coating.

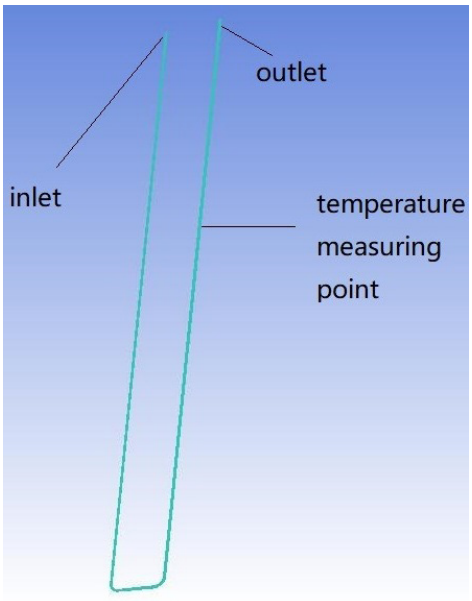

Figure 1. GK-VI tube reactor configuration.

MODEL DEVELOPMENT AND IMPLEMENTATION

Grid division and flow model

Because of structural similarity, only a representative tube of the industrial cracking furnace is simulated. The reactor is of the U-type as shown in Fig. 1, which is vertically suspended in the center of the furnace. The meshed domain, created by ICEMcfd, comprises 0.9 million cells, and the grid nodes have 1040420. The hexahedral cells are used to discretize the physical zone. The edge length of the smallest elements is 30 μm. The fluid flow, heat transfer and composition inside the reactor are obtained by solving the continuity equation, the momentum, energy and species conservation equations, and the turbulence kinetic energy and dissipation rate of turbulent kinetic energy equations with the commercial CFD package ANSYS FLUENT 14.0. The calculation of the three-dimensional turbulent flow field in the steady state is based on the solution of the Reynolds-averaged Navier-Stokes (RANS) equations in compressible formulation, closed with the standard κ-ε model (Tao, 2001).

Surface reaction model

At steady state, the coating deposition is balanced by the surface reaction. The TEOS CVD system has been focused on by many researchers (Coltrin et al., 2000; Daniel et al.,2015; Haupfear et al., 1994; Kim and Gill, 1995). Detailed surface reaction mechanisms for TEOS pyrolysis to SiO_2 have been reported based on the reactor-scale experiments or simulations (Coltrin et al., 2000; Daniel et al., 2015). Briefly, TEOS undergoes step-wise decomposition to form gas intermediates mainly by for-center molecular decomposition and C-C bond cleavage of the ethoxy branches. The activated species adsorb on the surface and later decompose into SiO_2. However, this process proceeds via a complex network of reactions and involves dozens of $Si_xO_yH_z$ intermediates (Coltrin et al., 2000; Daniel et al.,2015). Using the full reaction mechanism in the modelling including a three dimensional flow is impractical and unnecessary when considering that the simulation is on an industrial scale. In addition, the SiO_2 surface chemistry in the TEOS system on an industrial scale is different from that on a reactor scale. The distribution and adsorption of intermediates will be influenced by the residence time, surface conditions and temperature profile in a CVD reactor. Deposition of S involving a DMDS CVD system is a similar situation. Therefore, a simplified one-step reaction mechanism is adopted according to our previous study (Wang et al., 2013). In this mechanism, $Si(OH)_4$, H_2S, CH_3SH and CH_3SCH_3 are proposed to be the final Si/S-containing intermediate products of the decomposition of TEOS and DMDS before entering the tube reactor according to the thermodynamic calculation (Wang et al., 2013). The surface reaction schemes and kinetic parameters are shown in Table 2.

The validation and limitation of the surface reaction schemes and kinetic parameters have been discussed in our previous study, and the models used in Table 2 were in good agreement with the pilot scale test (Wang et al., 2013). In Table 2, E_a for Si deposition is chosen based on the apparent activation energy of the SiO_2 growth rate in a hot-wall TEOS system, and in S deposition they are based on the apparent activation energies for related sulfide pyrolyses (Wang et al., 2013). Therefore, the schemes present the apparent reactions correlating gas intermediates and coating deposition rates. Considering the simulation complexity of the detailed surface reaction and the study on an industrial scale, we think that the numerical model adopted in the present study is reasonable.

Physical properties

For the species inside the reactor, the kinetic theory is used to compute the viscosity, heat capacity and

Table 2. Arrhenius kinetic forms for surface reactions (Wang et al., 2013).

Surface reaction	Arrhenius equation	Reaction order
$Si(OH)_4 \rightarrow SiO_2 + 2H_2O$	$k = 2.0 \times 10^4 \exp(-138138/8.314T)$	1.0
$CH_3SCH_3 \rightarrow C_2H_6 + S$	$k = 2.2389 \times 10^{11} \exp(-196648/8.314T)$	1.5
$CH_3SH \rightarrow CH_4 + S$	$k = 3.02 \times 10^{13} \exp(-280328/8.314T)$	1.0
$H_2S \rightarrow H_2 + S$	$k = 3.6 \times 10^8 \exp(-200832/8.314T)$	1.0

thermal conductivity of these species in the mixture (Wang et al., 2013; Reid et al., 1977; ANSYS, Inc., 2011; Hu et al., 2011). For the molecular transport, the kinetic theory is used to compute the binary mass diffusion coefficient for species i in species j. The diffusion coefficients of the species were defined as a function of temperature over the range of 800K~1300K (Wang et al., 2013).

Boundary conditions and numerical methods

The parameters of the mass flow, temperature, and mixture composition at the inlet of the reactor are used in this simulation (as shown in Table 1). The composition and flow rate of the coating precursors in the reactor coil are assumed to be equal to each other. The outlet boundary condition of the reactor is determined by the pressure outlet boundary, which originated from the operating conditions of the coating preparation. The standard wall functions were used as turbulent wall boundary conditions. The no-slip boundary condition was imposed at the reactor walls. The external tube skin-temperature profile is assigned as the tube skin boundary, which is obtained from the industrial measurement during the coating preparation process.

The governing equations in the reactor tube are solved sequentially using a control volume-based method. The SIMPLE method is selected for pressure-velocity coupling, and the second order upwind scheme is used to interpolate the variables on the surface of the control volume.

RESULTS AND DISCUSSION

Effects of coating preparation on TLEs

The cracking gas from the tube outlet was quenched in the TLE section to avoid the loss of olefins by secondary reactions and the coating preparation should not have any adverse effects on its operation. The outlet temperatures of the three TLEs were monitored during the coating preparation process for evaluating the operating conditions of the TLEs. Meanwhile, the exhaust gas was sampled at the outlets of TLEs every 2 hours. The concentrations of sulfur and silicon in the condensate of exhaust gas were analyzed using Inductive Coupled Plasma Emission Spectrometer Atomic Emission Spectrometry (ICP-AES) and a Sulphur Analyzer (ANTEK-9000NS).

The results of the concentrations of silicon and sulfur in the exhaust gas are given in Table 3. It can be concluded that most of the coating precursors had been consumed in the cracker in all the tests by comparing the mass concentration of the precursors at the inlet with that at the outlet. However, the preparation processes influenced the operation of the TLEs. The profiles of the outlet temperature of the TLEs with time in the preparation process are shown in Fig.2. In test 1,

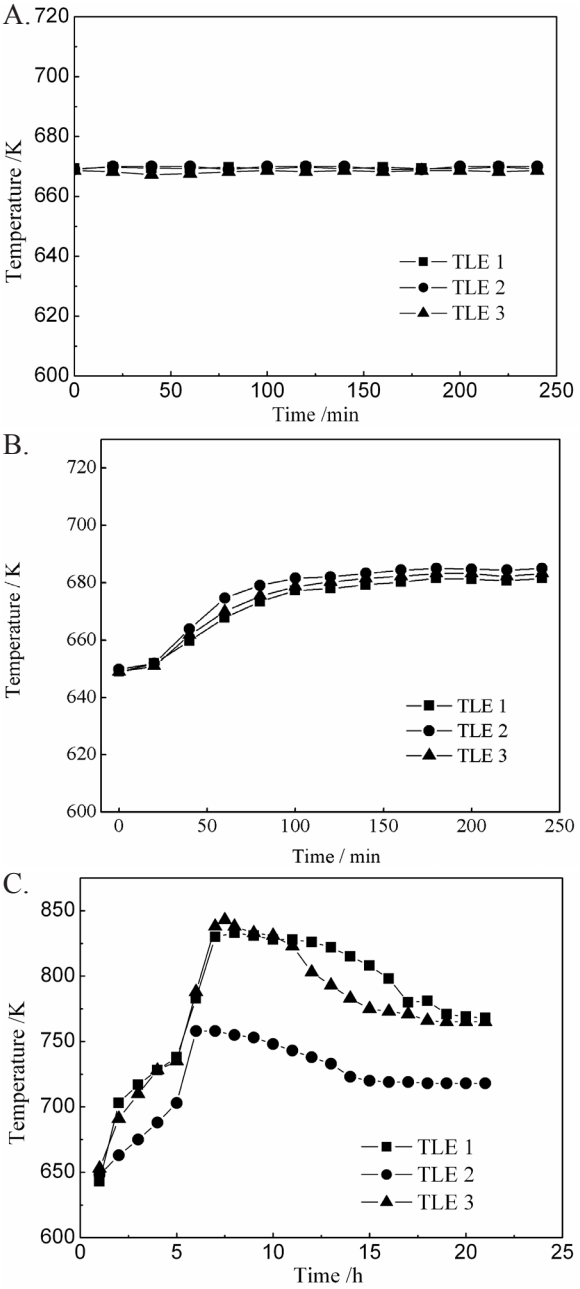

Figure 2. Profiles of the outlet temperature of the TLEs with time during the coating preparation. (a) Test 1; (b) test 2; (c) test 3.

Table 3. Concentrations of sulfur and silicon in the condensate of exhaust gas.

Elements	Test 1		Test 2		Test 3	
	2h sample	4h sample	2h sample	4h sample	2h sample	4h sample
Si(mg/l)	<0.5	<0.5	0.583	0.556	0.634	0.662
S(μg/g)	<0.5	<0.5	<0.5	<0.5	<0.5	<0.5

the on-line coating preparation had almost no adverse effects on the TLEs (see Fig.2a). In test 2, the outlet temperatures of the TLEs were raised about 25-35K in the first 100 minutes during the coating preparation when the flow rate of the coating precursors was appropriately adjusted to 100L/h and the preparation temperature was raised 10K (see Fig.2b). When the coating precursors were added at the rate of 150L/h, the outlet temperatures of TLE1 and TLE3 reached 848K in the first 8 hours (Fig.2c). The temperature exceeded the upper limit temperature, according to which the TLEs should be decoked at once, but the temperatures decreased from 848K to 763K in the next 12 hours.

The profiles of the outlet temperature of the TLEs with time indicated that the flow rate of the coating precursors had a main effect on the operation of the TLEs. The reported studies on the pretreatments with silicon or sulfur-containing additives under the TLE conditions are very limited. The coating preparation process was endothermic overall, involving the reactions of the thermal decompositions of TEOS and DMDS and the formation of the surface coating (Ho and Melius,1995; Wang et al.,2013). So the temperature increases at the outlets of the TLEs in test 2 and test 3 were mainly due to the decreased cooling effects of the TLEs. During the coating preparation, the coating precursors were introduced into the steam and decomposed when transported in the steam. Then the decomposed intermediates were adsorbed on the inner surface of the reactor coil to form the coating by a series of surface reactions. Essentially the pretreatment was a chemical vapor deposition (CVD) process. The integrity and quality of the coating prepared by the CVD method, including the morphology, the thermal stability property, and the hardness and tensile strength, were greatly affected by the deposition temperature (Ho and Melius,1995; Zhou et al.,2008). Coating precursors would also be transported into the TLEs by the steam carrier. The precursors/steam mixture came out from the radiant tubes at about 1073K and were cooled to about 673K in TLEs. In the TEOS CVD process, the thermal decomposition of TEOS involves different mechanisms depending on the temperature (Haupfear et al., 1994; Kim and Gill, 1995). The apparent activation energy for cold-wall deposition studies was found to be 21.5±3.8 kcal/mol while it was above 36 kcal/mol for hot-wall kinetic data (Kim and Gill, 1995; Raupp et al.,1992). With regard to the formation of a SiO_2 layer with stable thermophysical properties and better film quality, the pretreatment with TEOS should be carried out at above 700°C (Adachi et al., 1992; Kim and Gill, 1995; Wang et al., 2007). Many researches involving TEOS/SiO_2 system have also found a kind of powder deposit generated mainly by homogeneous nucleation in the pipeline after the reactor (Adachi et al., 1992; Delperier et al., 1988). Therefore, it is reasonable to believe that a kind of deposition product had been formed from both homogeneous nucleation and fast heterogeneous reaction, and piled up on the internal surface of coils under the TLE operating temperature. This kind of deposition did not possess the mechanical and thermophysical properties that the SiO_2/S coating had because of the reduced deposition temperature in the TLE (Zhou et al., 2011). As a result, the deposition with less densification of the internal structure could be washed away gradually by the cracking gas and was carried further downstream (see Fig.2c). To support our assumption, the deposited residues were sampled in the TLE in a pilot-scale test. The outlet temperatures of the tube reactor and TLE in the pilot-scale test were 850 °C and 430 °C (Zhou et al., 2011). The mass concentration of precursors was kept at 0.2-1%. Figure 3 shows the deposition of this kind collected after the coating preparation in the TLE. The deposits had broken into fragments in the figure, presenting a lower densification texture (see Fig.3a). Meanwhile, this coating, composed of small particles, had a similar micro surface structure (see Fig.3b) to that deposited in the radiant coil. The deposits may also be formed in the pipeline section. But as the concentrations of Si at the TLE outlet are below 1ppmw in all tests (see Table 3), it is believed that the deposits were mainly formed in the TLE section.

Effects of on-line coating on coke formation and main product yields

Microscopic analysis of inner wall of 8-year-served HP40 tube and on-line coating

The reactor tube is made of 35Cr45Ni steel (35Cr, 45Ni, 0.45C), and the service life is about 64,000 h (8-year-served) at an elevated temperature. Figure 4 shows the microstructure of the inner wall of the reactor tube cut from the tube outlet before the coating tests. In a cracking furnace, the cracking tube is contacted by variable cracking and decoking gases in the high temperature condition, which leads to the formation of an oxide scale on the inner surface (Gandarillas et al., 2014; Olahova et al.,2018). As seen in Fig.4(a), the inner surface shows an etched morphology. This mainly results from periodic spalling and regeneration of the oxide scale (Liu and Chen, 2011; Wu et al., 1998). Fig.4(b) indicates that the oxide scale mainly consists of Cr, Mn, Fe, Ni, and Si elements. Calcium may come from air and from de-ionized water (Zhou et al., 2007). Fig.4(d) is the result of EDS linear scanning of the cross section. Clearly, the external oxide layer close to the surface (marked “A”), with a thickness of approximately 20 μm, is rich in Cr and O, but depleted in Ni and Fe. In the temperature range 800-1050 °C the usual heat-resistant materials with high Cr content

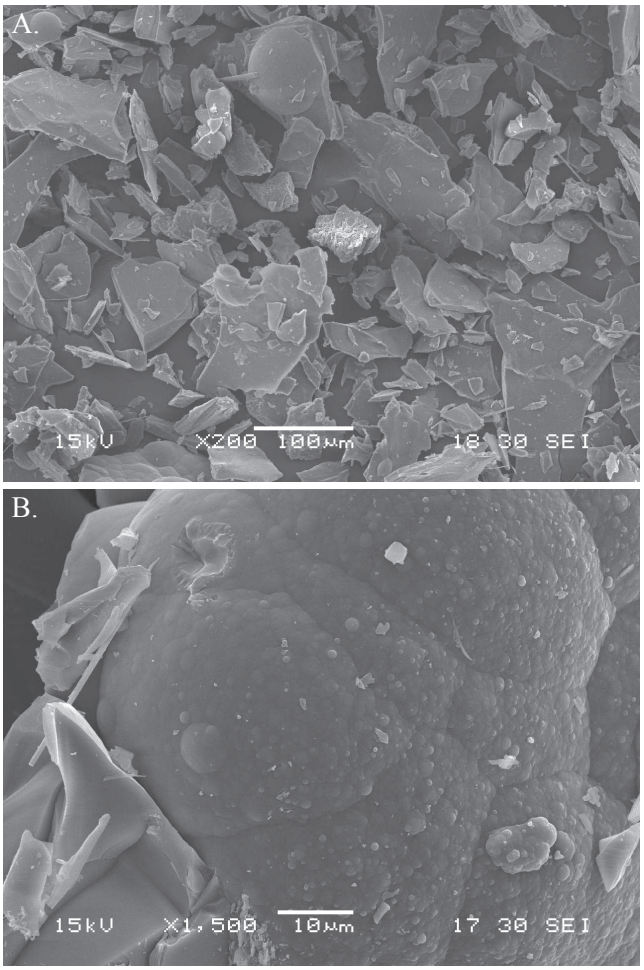

Figure 3. Deposited residues in the TLE in the pilot-scale test. (a) Magnification×200; (b) magnification×1500.

will form an outer oxide scale on the surface, mainly composed of Cr-containing compounds, e.g., spinel (Mn, Fe)Cr_2O_4 and chromia Cr_2O_3, which can protect the substrate from carburization because of the low carbon solubility in the oxide (Wang et al., 2007; Wang et al., 2008). The loss of Fe and Ni elements in the external scale are due to oxidation and oxide spallation in cracking/decoking cycles (Grabke and Jakobi, 2002). A decrease of Cr in the internal oxide scale (marked "B") is also observed in Fig.4(d). For the Fe-Ni-Cr alloy tube, periodic spalling and regeneration of the external oxide scale consume chromium in the substrate and lead to the outward diffusion of Cr to the surface continually. But the low diffusivity of Cr in the alloy will result in a chromium-depleted zone below the oxide scale (Grabke and Jakobi, 2002; Wu et al., 1998). The chromium-depleted zone widens with increasing the service life of the cracking tube (Wu et al., 1998). In Fig.4(c), the intrusions of heavier oxides into the matrix metal (marked "B") are also be observed. The EDS line analysis of Cr, Si, O elements in the range of 80-120 μm indicates that the oxides are

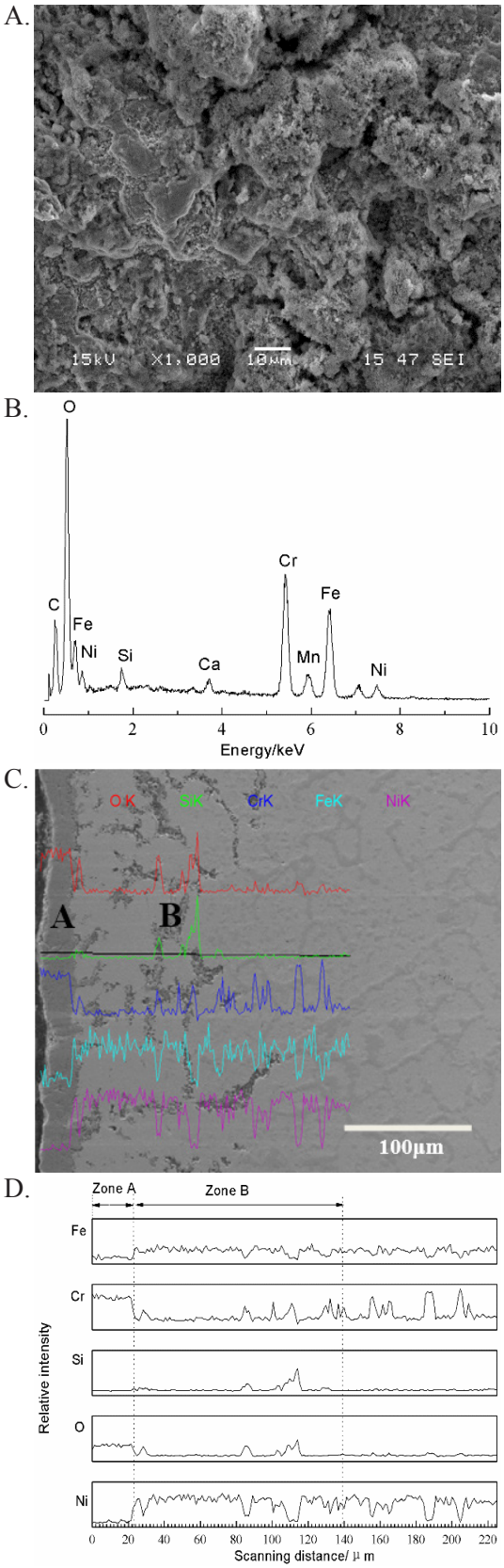

Figure 4. Microstructure of the tube reactor on the inner surface. (a) Morphology of the inner surface; (b) EDS analysis of the inner surface; (c) cross section of the reactor tube; (d) EDS linear scan of the cross section.

composed of silica and chromia. In Fe-Ni-Cr cracking tubes, silicon is always included in small amounts and is well known to tend to aggregate beneath the oxide layer in the form of internal silicon oxide (Gandarillas et al., 2014). Song and Wu (Song and Wu, 2018) analyzed the microstructure characteristics of a Cr35Ni45 cracking tube with the service life of about 52,000h. They revealed that a continuous chromium-rich oxide layer (external oxidation) with a thickness of about 40μm along with a discontinuous silicon-rich oxide layer (internal oxidation) formed on the inner surface. The elemental distribution in the inner surface region in our study is consistent with the research results for a Fe-Ni-Cr alloy tube after long term service (Pourmohammad et al. 2019; Song and Wu, 2018).

Two cracking runs were followed after test 1. A sample was cut from the reactor coil at the outlet. Figure 5(a) shows that the surface of the inner wall is not completely covered by the coating. The coating most probably has spalled from the inner surface in the cracking/decoking conditions. In Figure 5(b), it is found that the coating exists in the cavities at the surface. The cross section of the inner wall shows the interface with a jagged configuration (Fig.5(c)), at which the coating has been deposited (Fig.5(d)). Generally, an interface with a complicated geometric

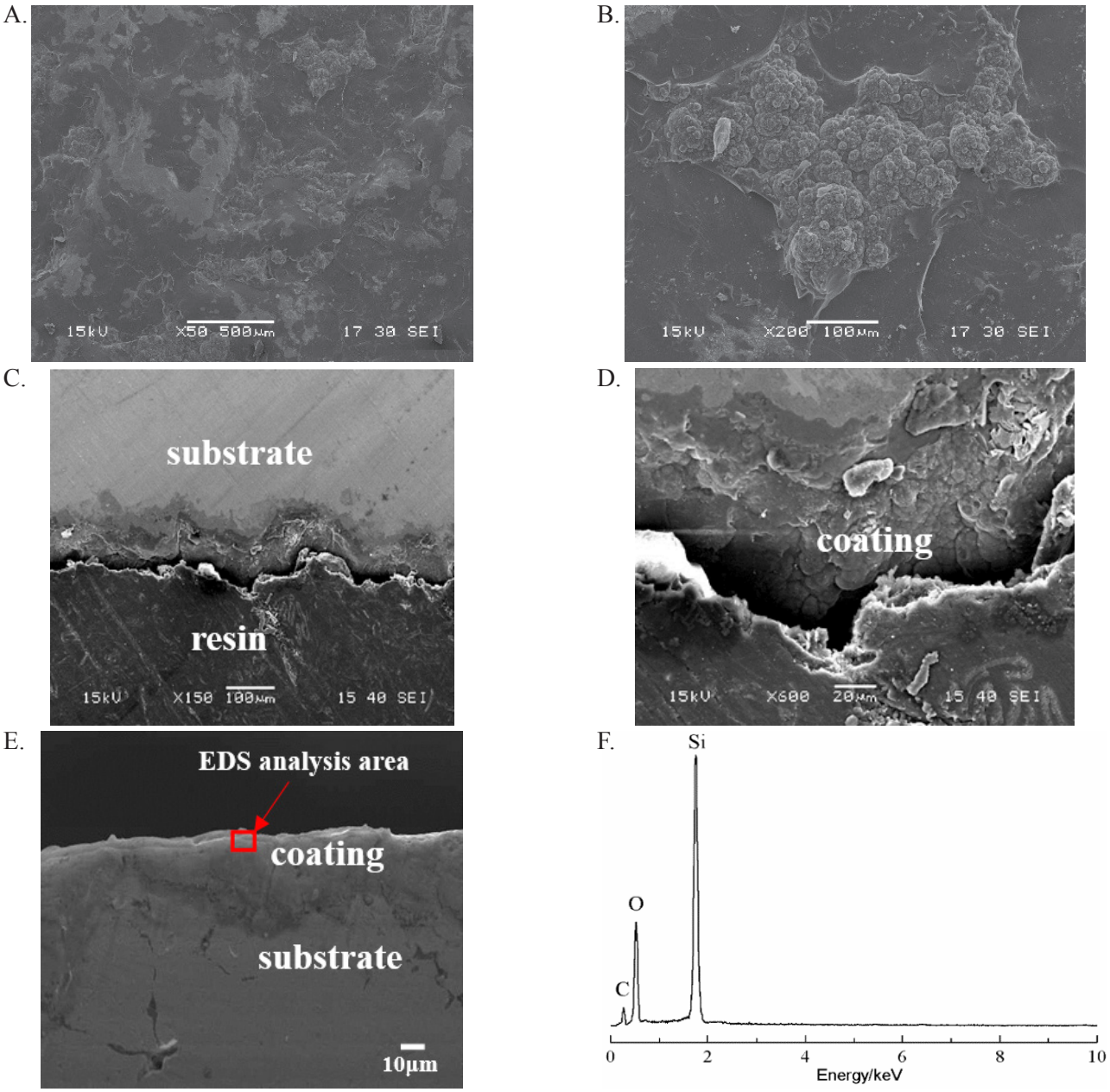

Figure 5. SEM analysis of the inner wall and the cross section of the reactor tube after test1 followed by another two cracking runs. (a) Inner surface of the reactor tube; (b) coating in the cavities; (c) cross section of the interface; (d) coating deposited at the interface; (e) cross section of the coating; (f) EDS analysis of the coating.

configuration can improve the mechanical binding between the coating and the substrate. In Fig. 5(e) and (f), EDS analysis of the area located close to the top surface confirms the coating deposition at the interface. However, the content of S is too low to be detected by EDS. On the one hand, S is designed to be a minor element in the coating so that DMDS is only added in a low range of 5-20 ppmw. On the other hand, the volatilization from the coating during the subsequent cracking process will also result in a very low content of S in the coating.

Evaluation of the on-line coating for coking inhibition

In a cracking furnace, the growth of the coke layer with running time leads to an increased heat resistance. The effects are compensated for by increasing the heat input to the cracking tube continuously to retain the same process temperature and hence the same conversion. Therefore, the tube metal temperature (TMT) increases with the running time, and the furnace is taken out of production for the decoking operation when TMT reaches the maximum operation temperature (MOT) of the coil tube. TMT is always an index of evaluating the coking quantity, and the change in the trend of TMT over the run time can be used to study the coking rate qualitatively in industry (Cai et al., 2002; Sadrameli, 2015). The coking tests were carried out under the same cracking conditions for both the blank run and the test runs, which are listed in Table1. Because the decoking conditions were the same, the external tube skin temperatures in all the cases could be thought to be approximately same or to be similar at the start of the cracking run.

The profiles of TMT with cracking time are presented in Figure 6. It is found that the increasing rate of the TMT for the blank run is fast in the first 3 days, indicating a high initial coking rate, and then decreases and reaches a stable value in the next 10 days.

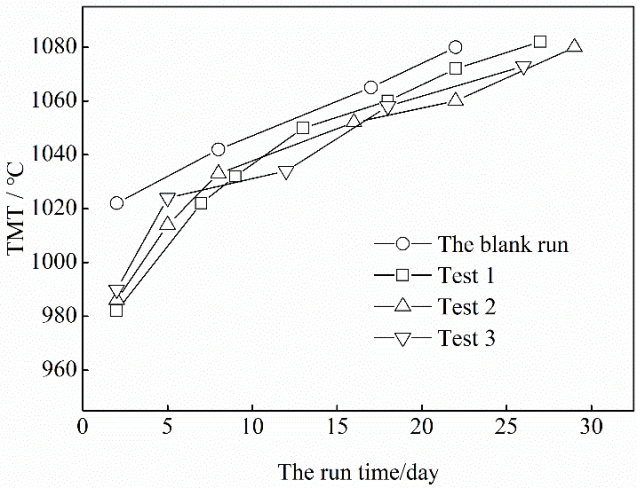

Figure 6. Profiles of TMT with cracking time in industrial tests.

The increasing rates of TMT for the three test runs in the first 3 days are lower compared to the blank run, indicating decreased initial coking rates. The profiles of TMT of the three tests have the similar trend in the next 20 days. The run length was 22 days for the blank run, while it was 26-29 days for the three test runs.

Generally, the high coking rate at the beginning of the cracking run is due to the catalytic activity of nickel and iron on metal surfaces. Specially, the initial coking rate is always higher for the long-term-served cracking tube coil. In a long-term-served cracking furnace, the cracking tube is not only subjected to high temperature, but is also in contact with variable reducing/oxidizing atmospheres and periodic cold/heat fatigue or heat vibration, which lead to the change of the surface conditions compared to the new tube. So a tube after a long-term service generally presents a higher catalytic coking rate because of significant populations of catalytic sites (Wu et al., 2001). The TMT profiles in the first about 5 days in Fig.6 mean that the blank tube had a higher catalytic coking rate than the coated tubes. With increasing time on stream, the metal surface is encapsulated by coke, and the catalytic activity of the metal decreases. The main route for coke formation is taken over by the heterogeneous noncatalytic mechanism, which leads to a constant so-called asymptotic coking rate (Wang et al., 2007). In Figure 6, the TMT increases steadily for the blank in the next about 20 days, which may represent this process involved. Similarly, the TMT profiles of the coating tests show the gradual increase in temperature after about the first 5 days. Based on the analysis above, it can be stated that the on-line coating reduced the coke formation mainly by decreasing the catalytic coking. The run time of the coated tube was hence prolonged.

It is worth noting that the effectiveness of the coating to reduce coke formation is very limited. This is because the coating could only suppress the formation of catalytic cokes by passivating the tube wall to reduce the metal activity without altering the microstructure of the coke layer. Under the operating conditions in an industrial cracker, the initial rate only has a smaller contribution to the final coke formation during the run length because the largest amount of coke formed results from the heterogeneous noncatalytic coke formation (Zhou et al.,2007). Therefore, the coking inhibition effect of the coating applied in an industrial cracker is less significant as compared to that in a pilot-scale setup. Moreover, the initial coking rates are higher during gas feed cracking, while higher asymptotic rates are observed in naphtha cracking (Gandarillas et al., 2014). Our next work is to apply the on-line coating in a small-sized cracker or the cracker using gas feed. The test results indicate that the on-line coating can be applied

in a long-term-served industrial cracking furnace for coking inhibition, which provide more flexibility to the ethylene producers when compared to the off-line coating technology.

The effects of the SiO_2/S coating on the main product yields were also evaluated. The cracking gas was sampled every 15 days for test 1 and test 2. The results of the main product yields in the industrial furnace with the application of the coating, together with those of the blank run, are summarized in Table 4. It is found that the application of the on-line coating did not have a significant influence on the distribution of products and the molar yields of main products were only marginally influenced. The slight change of the molar yields of hydrogen may be due to the effect of the coating application, which influences the dehydrogenation of hydrocarbons by catalytic metals at high temperatures.

Table 4. Main product yields of naphtha cracking in the industrial cracker (mol. %).

Composition	Test 1		Test 2	
	Blank	Coating	Blank	Coating
H_2	15.33	14.01	14.61	13.25
CH_4	28.40	28.20	28.82	29.38
C_2H_2	0.58	0.60	0.64	0.61
C_2H_4	32.88	33.48	33.68	34.22
C_2H_6	3.83	3.81	3.49	3.82
C_3H_4	0.24	0.25	0.45	0.43
C_3H_6	10.84	11.10	10.92	11.22
C_3H_8	0.35	0.35	0.32	0.32
C_4H_6	3.61	3.76	2.68	2.57
C_4H_8	0.63	0.66	0.58	0.61
C_4H_{10}	0.18	0.2	0.09	0.11
1-C_5H_{10}	1.12	1.40	1.48	1.42
C_6	0.59	0.74	0.74	0.71

REACTOR SIMULATION AND ANALYSIS

Intermediate mass fraction and deposition rate profiles

The simulations were conducted first to validate the model adopted by us based on the conditions of test 1. Fig.7 illustrates the profiles of intermediate mass fraction and deposition rate along the reactor tube. As S is designed to be present in a small amount in the coating (about 1% of the mass content) in industry, it is proposed that the physical properties of the coating are equal to amorphous SiO_2 (Wang et al., 2013) For test 1, the coating thickness at the outlet is approximately 62μm according to the simulation based on the relationship between the coating thickness and the deposition rate:

$$\delta = \frac{R_{dep} t}{\rho_{coating}}$$

where t the deposition time length, $\rho_{coating}$ the density of amorphous SiO_2, δ the coatings thickness and R_{dep} the

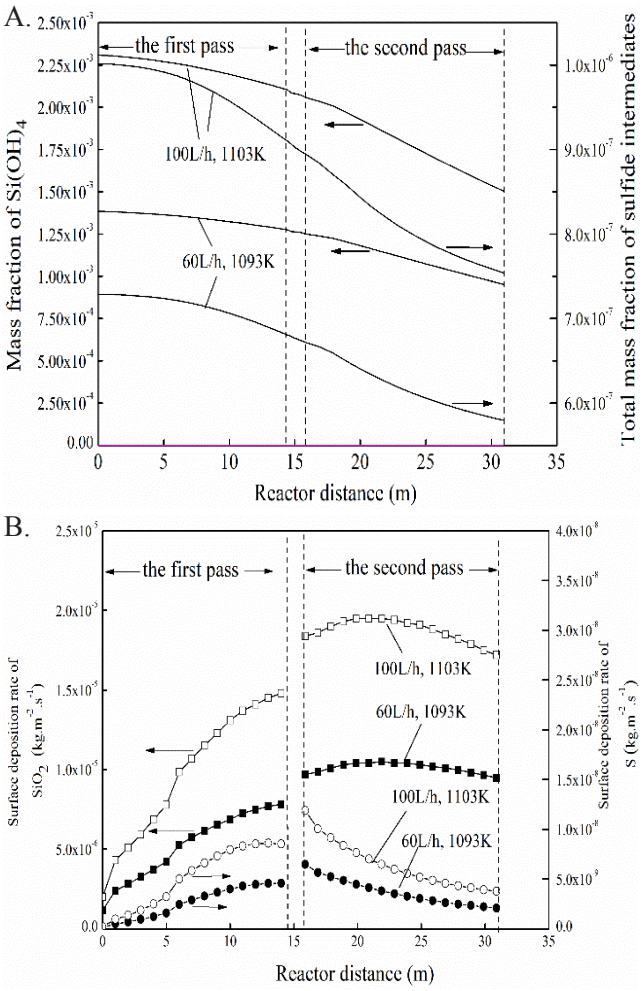

Figure 7. Profiles of intermediate mass fractions and deposition rate along the reactor tube. (a) Mass fractions of Si/S-containing intermediates; (b) deposition rates of SiO_2 and S.

deposition rate. It is shown that the calculated result has the same magnitude as the test 1 thickness of about 30-50 μm (see Fig.5(d)). No S was detected in the coating by energy dispersive spectroscopy (see Fig.5(f)). However, a very weak peak of Si-O-S structure at around 553cm^{-1} was detected by Raman spectroscopy. The calculated results also confirm the low mass ratios (about 0.08%) between S and SiO_2 at the outlet and the S content is below the detection limit of EDS In addition, S will be lost from the coating because of the volatilization under the cracking conditions (Olahova et al., 2018). The reason for the selection of surface reaction schemes has been explained in the above section "Surface Reaction Model". The validation and limitation of these surface reactions have been discussed in our previous study, and the models used in Table 2 were in good agreement with the pilot scale test (Wang et al., 2013) Considering the simulation complexity for the detailed surface reaction and the study on an industrial scale, we think that the numerical model adopted in the present study is reasonable.

The mass conversion rates of $Si(OH)_4$ are 31% and 35% for test 1 and test 2. For sulfide intermediates, the mass conversion rates are 20% and 25%, respectively. The gas velocities in the tube are in the range of 100-150m/s based on the simulation. It is noted that the low residence time of about 0.2 s in an industrial reactor leads to low conversion rates of Si/S-containing intermediates, especially for sulfide intermediates. The deposition rates of SiO_2 increase along the reactor tube in the two tests, and the maximum rate is found at about 23 m of the length of the tube. For S, the deposition rates increase along the first pass tube, and then decrease along the second pass. In test 1, the coating thicknesses are in the range of about 7-51μm in the first pass, obtained from Equation (8), and in the range of 63-68μm in the second pass. In test 2, the coating deposition rates are about 2 times those in test 1.

In the tests, the mass fraction of S in the coating is in the range of 0.05%-0.1% in the straight tube sections. The deposition of S is much smaller than SiO_2 as S is designed intentionally as a minor element in the coating. In a SiO_2/S coating, S breaks the Si-O-Si bonds in the silica network matrix and promotes the formation of a three-membered ring Si-O-Si structure, which has good thermal stability at the cracking temperature (Zhou et al., 2007). In the pilot-scale test, the mass content of S in the coating is about 3-5% (Wang et al., 2013). For the industrial furnace involving naphtha feed cracking, a large dose of DMDS is always applied to presulfide the reactor surface. In our tests, the low concentrations of DMDS are chosen in the range of 5-20 ppmw relative to the steam based on the consideration that the sulfur concentration in straight run naphtha usually ranges from 20 to 100 ppm (Gandarillas et al., 2014). S contained in the naphtha is then added into the coating in the subsequent cracking process, and the behavior of S addition may continue for several days until the coating is completed covered by coke layers.

The surface Damkohler number (Da_s) is expressed as (Kleijin, 2000)

$$Da_s = \frac{R_s \delta_b}{DC}$$

where R_S is the surface reaction rate, δ_b the thickness of the boundary layer, D the diffusion coefficient of the intermediate species, and C the concentration of intermediate species at the thickness of the boundary layer. A large number (>>1) indicates that the control step of the CVD process is the mass transports of intermediates to the surface through the boundary layer, and a small value means a surface reaction limited process. The thickness of the sublayer δ_b, can be obtained from (Wang et al.,2013)

$$\delta_b = 5\frac{\nu}{u^*}$$

The Damkohler numbers for the deposition of SiO_2 and S calculated from Equation (1) are of the order of magnitude of 10^{-3}-10^{-1}, indicating that the surface reaction limits the deposition process.

Influence of flow rate

The parameters influencing the coating deposition rate include the temperature, the steam flow rate and the concentration of coating precursors. In an industrial furnace, the adjustment of COT is careful in case of damage of tube materials. The adjustment of the concentration should also be cautious as the deposits formed have an effect on the downstream section. In this section, the influence of steam flow rate on the deposition was numerically studied in order to obtain the optimized condition of coating preparation. In the simulations, the thermal boundary conditions were simplified as no industrial measurement was carried out and the inlet mass fraction of intermediates were kept the same as in test1. The simplified external tube skin-temperature profile is described by the equation:

$$Q_{wall} = \sigma AF\left[T_{flue\ gas}^4 - T_{wall}^4\right]$$

The flue gas temperature is set to be 1093K throughout the furnace, under the condition of which the process gas temperature increases gradually along the reactor and reaches 1093K. The simplified thermal boundary conditions are adopted for the purpose of investigating the coating deposition process without being affected by the factors which should be considered in coupled furnace/reactor simulation. For example, significant circumferential differences in tube skin temperature around the tube perimeter were found because of the presence of "front" and "shadow" sides on the tubes when the furnace and the reactor were coupled (Van Geem et al., 2004).

Fig. 8 presents the profiles of intermediate mass fraction and deposition rate when the flue gas temperature is 1093K. The mass conversion rates of $Si(OH)_4$ are 61%, 43% and 22% when the flow rates are 10 t/h, 15 t/h and 25 t/h. For sulfide intermediates, the conversion rates are 30%, 24% and 17%, respectively. The deposition rates of SiO_2 present monotonic trends along the 2 tube passes, respectively, especially for low inlet flow rate. The higher deposition rates for 10t/h along the first pass are attributed to higher wall temperatures because of the lower inlet flow rate at the same flue gas temperature. The deposition rate of S decreases along the second pass. For 10 t/h, the S deposition profile shows a crest along the first pass. However, increasing the flow rate accelerates the transport of intermediates and the enhancement of mass transfer gradually eliminates the deposition crest at the first pass. The flow rates of 15 t/h and 25 t/h give similar S deposition rate profiles in the second pass.

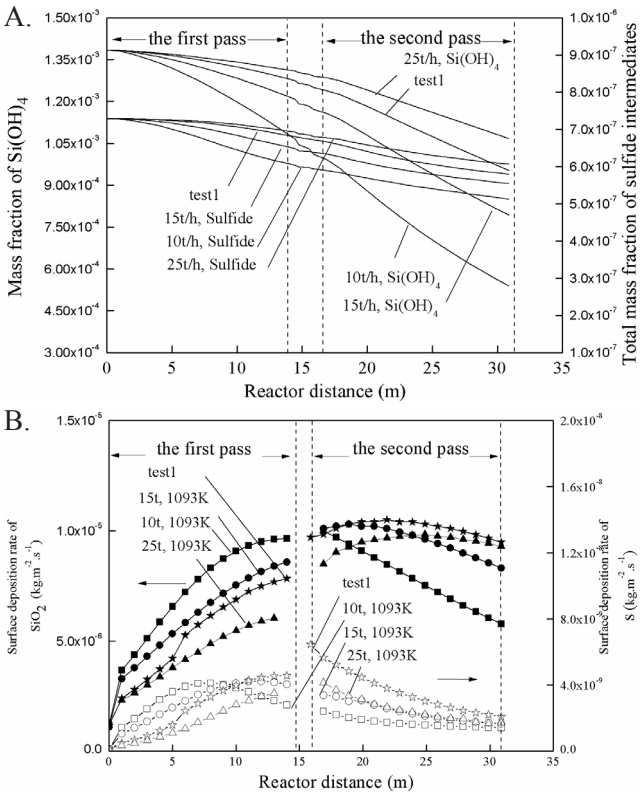

Figure 8. Profiles of intermediate mass fractions and deposition rate along the reactor tube at different flow rates. (a) Mass fractions of intermediates; (b) deposition rates of SiO_2 and S.

It is noted that a high flow rate gives a more uniform thickness and improved mass content of sulfur in the coating in the second pass, where the coking rate is always high. For the inlet flow rates studied, the mass fraction of S of the coating in the straight tube sections increases when increasing the flow rate, but still within a low range of 0.02%-0.1% .

At the tube bend, the mass fraction profiles of intermediates show small fluctuations, mainly caused by the irregular flow pattern in the bend where the axial flow is pushed toward the outer wall due to centrifugal forces. Figure 9(a) shows the velocity at the reactor distance of L=15.116 m where the diameter has changed. It reveals that there exist strong radial nonuniformities of the velocity at this position. Similar profiles are also observed for the mass fraction of $Si(OH)_4$ and temperature illustrated in Fig.9(b) and Fig. 9 (c). The radial velocity nonuniformities lead to a low temperature zone close to the outer wall as the circumferential difference in heat absorption at the same flue gas temperature.

Figure 10 shows the coating deposition rate profile at four circumferential positions. For the four curves, obvious circumferential nonuniformities for the deposition at the bend are found due to circumferential differences in the temperatures and mass fractions. Along the tube bend, the maximum circumferential

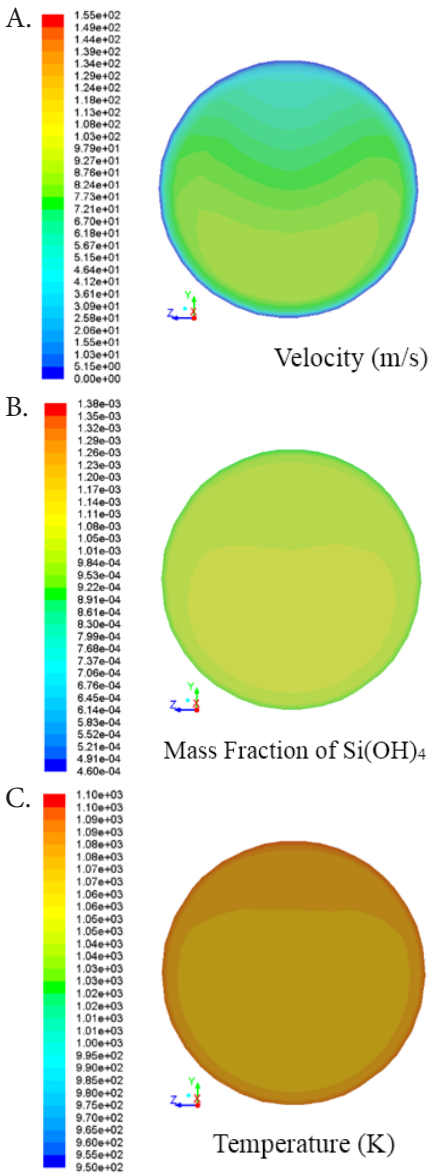

Figure 9. Radial profiles of (a) velocity, (b) mass fraction of $Si(OH)_4$ and (c) temperature at a reactor distance of L = 15.116 m.

temperature difference of 8 K has been simulated (see Fig.10(a)). The highest temperature position "C" among the four positions gives the highest deposition rate of SiO_2 although it also corresponds to the lowest mass fraction position (see Fig.10(a) and Fig.10 (b)). However, the deposition at "C" gradually reaches the minimum value among the four positions at the end of the tube bend and the difference in circumferential temperature remains at about 5 K. The lower concentration of $Si(OH)_4$ at "C" compared with those at the other three positions is responsible for the deposition rate decline. S deposition at four circumferential positions presents similar profiles along the bend.

Figure 11 further shows coating deposition rate profiles at different inlet flow rates along the tube

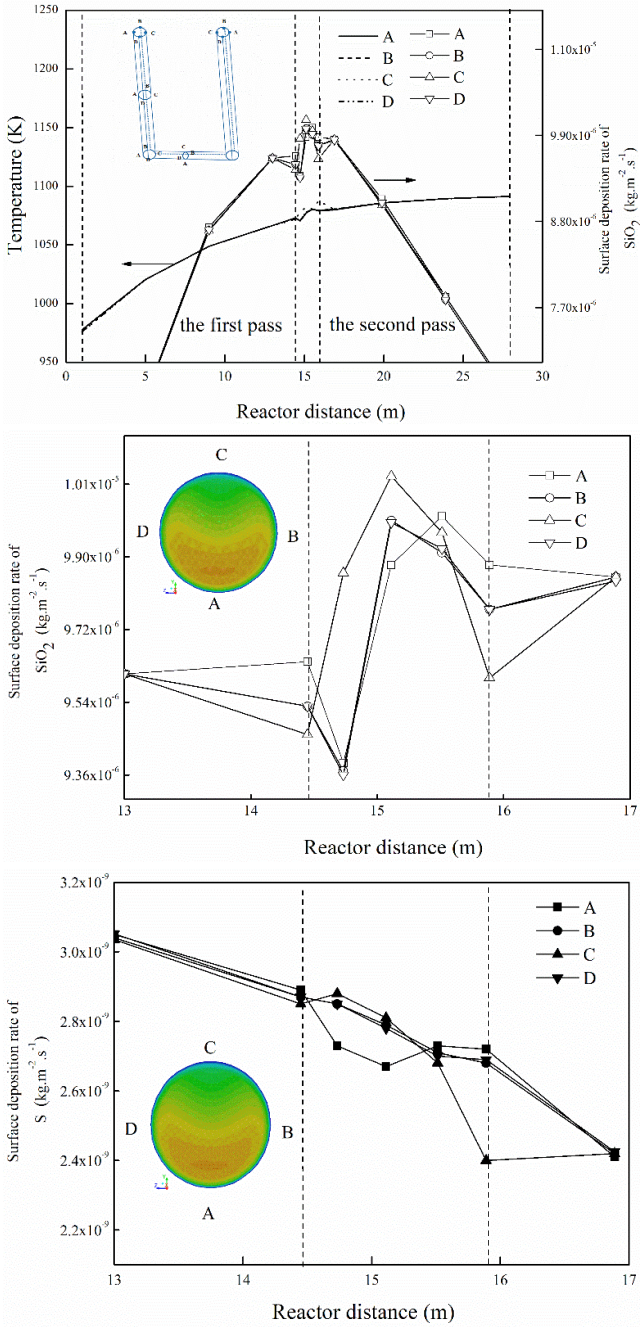

Figure 10. Profiles of temperature and coating deposition rate along the reactor tube at an inlet flow rate of 10t/h. (a) Profiles of temperature and SiO_2 deposition rate; (b) profile of SiO_2 deposition rate along the tube bend; (c) profile of S deposition rate along the tube bend.

bend. For the inlet flows of 15 t/h and 25 t/h, the maximum circumferential temperature differences are about 9 K and 15 K (not shown here). Fig.11 confirms that the contribution of temperature to the deposition at "C" overcomes the concentration of intermediates with increasing flow rate. Hu et al. (2011) found circumferential differences in coking rates in the tube bend section due to the irregularities in the flow

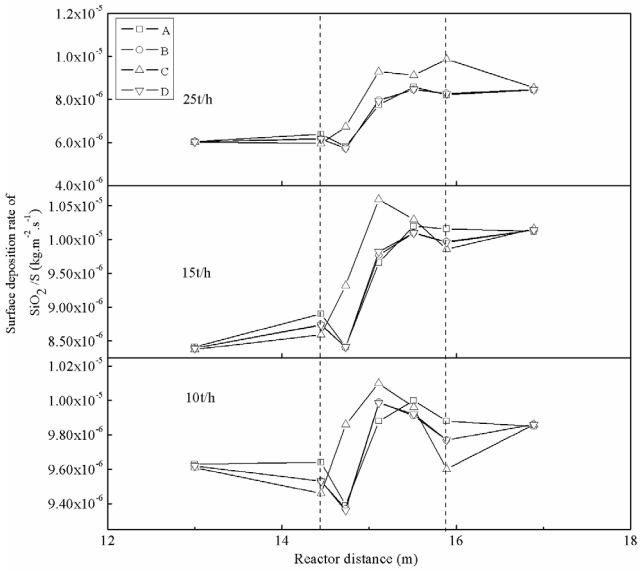

Figure 11. Profiles of the coating deposition rate along the tube bend.

pattern. The highest coking rate position among the four circumferential positions corresponded to the side of the cross section with the higher ethylene weight fraction (Hu et al., 2011). Our simulation results indicate that it is hard to improve the circumferential uniformness of coating thickness by changing the inlet flow rate in the tube bend section. In addition, the positions with high coking rates do not just match the positions with high coating deposition rates. The location with the highest coating deposition rate circumferentially may correspond to the one with the highest coking rate or the lowest. The mass content of S in the coating is about 0.03%-0.05%.

Coating preparation optimization

For a long-term-served cracking tube, an on-line coating with a certain thickness is necessary so the coating could completely cover the rough surface. Generally, the surface roughness Rα for the ex-service tube can reach up to several tens of micrometers. The simulation results above indicate that it is necessary to maintain a high inlet flow rate in the reactor to achieve an uniform thickness, especially in the high temperature section. Meanwhile, the high velocity improves the content of sulfur in the coating due to the enhancement of mass transfer in the straight tube section. However, higher velocity decreases the coating thickness in the first pass and has little effect on the S deposition rate in the second pass (see Fig.8). In addition, high velocity leads to low conversions of intermediates, which may cause more deposited residues in the TLEs. The inlet mass concentration of test 1 had little effect on the TLEs. Based on the results in test 1 and the simulation, the operating parameters, i.e., the inlet flow rate of 15 t/h, the outlet temperature of 1093K and the inlet mass concentration of 3000

ppm (wt. %), is suitable to prepare the on-line coating in an GK-VI furnace.

CONCLUSIONS

An on-line SiO_2/S coating is prepared on the inner surface of coils in an 8-year-served GK-VI industrial cracking furnace for inhibiting coking. The coking rates of the tube with and without coating preparation are evaluated. The effects of the preparation process on the operation of the TLE are also studied. To obtain reasonable operational conditions for the coating preparation, simulations of the coating deposition process are carried out using the computational fluid dynamics (CFD) approach. Comparison with the coating thickness in the industrial test shows that the simulation results are the same magnitude as the test results. Hence, the simulation model is adopted to further investigate the effects of inlet flow rate on the coating deposition rate. The simulation results are expected to provide a theoretical guide for industrial practice. The main conclusions are as follows:

(1) The concentration of coating precursors has important effects on the operation of the TLEs. The outlet temperature of the TLE even reached 848K when the concentration of coating precursors was 7500 ppm (wt. %), i.e., 150 L/h. The main reason for the temperature increase is due to the decreased cooling effects of the TLEs, which come from the accumulation of SiO_2 and S in a loose form in the TLEs under the rapidly decreased temperature conditions. Sulfur and silicon concentrations in the effluent gas are both less than 1 ppm during the preparation process, indicating almost complete consumption of the precursors in tubes and TLEs.

(2) The run time of the GK-VI cracking furnace after the coating preparation is extended by 4-7 days. The on-line coating reduces coke formation by decreasing the catalytic coking, without altering the structure of the coke layer. Therefore, the coking inhibition effect of the coating applied is less significant because of the lower contribution of the catalytic coking to the final coke formation in an industrial cracker. The on-line coating did not significantly influence the distribution of products and molar yields of the main products. The slight decrease of hydrogen in the molar yields may be due to the inhibited dehydrogenation of hydrocarbons when the coating is applied.

(3) In the first pass of the cracking tube, the coating deposition rates decrease with increasing inlet flow rate. In the second pass, increasing the inlet flow rate gives a more uniform thickness and improved mass content of sulfur in the coating. In the tube bend section, obvious circumferential nonuniformities for the deposition are found due to circumferential differences in the temperatures and mass fractions. Changing the inlet flow rate has little effect to retard the circumferential nonuniformities. The mass fraction of S in the coating is within in a low range of 0.02%-0.1%. The very low content of S is designed intentionally based on the consideration that S contained in the naphtha feed is added into the coating in the subsequent cracking process. Da numbers show that the control step for the SiO_2/S coating deposition is kinetic. The coating preparation parameters are optimized based on the simulation results in an GK-VI furnace, i.e., an inlet flow rate of 15 t/h, an outlet temperature of 1093K and an inlet mass concentration of 3000 ppm (wt. %).

ACKNOWLEDGEMENTS

The authors gratefully acknowledge the National Natural Science Foundation of China (NSFC) for supporting the present work under the Project (grant no. 21706159) and Sinopec Nanjing Yangzi Petrochemical Company Ltd. for supplying the industrial data.

REFERENCES

Adachi, M., Okuyama, K. N., Tohge, N., Shimada, M., Satoh J., Muroyama, M. Gas-Phase Nucleation in An Atmospheric Pressure Chemical Vapor Deposition Process for SiO_2 Films Using Tetraethylorthosilicate (TEOS). Japanese Journal of Applied Physics, 31, 1439-1442 (1992). https://doi.org/10.1143/JJAP.31.L1439

ANSYS FLUENT User, s Guide 14.0, Chapter 8, ANSYS, Inc., Canonsburg, PA , USA (2011).

Bao, B. B., Liu, J. L., Xu, H., Wang, Z. Y., Zhang, K., Fabrication of Spinel Coating on HP40 Alloy and Its Inhibition Effect on Catalytic Coking during Thermal Cracking of Naphtha. Brazilian Journal of Chemical Engineering, 35, 721-730 (2018). https://doi.org/10.1590/0104-6632.20180352s20160670

Cai, H., Krzywicki, A., Oballa, M. C. Coke Formation in Steam Cracker for Ethylene Production. Chemical Engineering and Processing, 41, 199-214 (2002). https://doi.org/10.1016/S0255-2701(01)00135-0

Coltrin, M. E., Ho, P., Moffat, H. K., Buss, R. J. Chemical Kinetics in Chemical Vapor Deposition: Growth of Silicon Dioxide from Tetraethoxysilane(TEOS). Thin Solid Films, 365, 251-263 (2000). https://doi.org/10.1016/S0040-6090(99)01059-7

Daniel, N., Buerger, P., Akroyd, J., Kraft, M. A Detailed Kinetic Study of the Thermal Decomposition of Tetraethoxysilane. Proceedings of the Combustion Institute, 35, 2291-2298 (2015). https://doi.org/10.1016/j.proci.2014.06.093

Delperier, B., Vinante, C., Morancho, R. Analysis and Modelling of Tetraethoxysilane Pyrolysis. Journal of Analytical and Applied Pyrolysis, 13, 141-149 (1988). https://doi.org/10.1016/0165-2370(88)80054-8

Gandarillas, A. E. M., van Geem, K. M., Reyniers, M.-F., Marin, G. B. Coking Resistance of Specialized Coil Materials during Steam Cracking of Sulfur-Free Naphtha. Industrial & Engineering Chemistry Research, 53, 13644-13655 (2014). https://doi.org/10.1021/ie502277e

Grabke, H. J., Jakobi, D. High Temperature Corrosion of Cracking Tubes. Materials and Corrosion, 53, 494-499 (2002). https://doi.org/10.1002/1521-4176(200207)53:7%3C494::AID-MACO494%3E3.0.CO;2-T

Haupfear, E. A., Olson, E. C., Schmidt, L. D. Kinetics of SiO_2 Deposition from Tetraethylorthosilicate. Journal of the Electrochemical Society, 141, 1943-1950 (1994). https://doi.org/10.1149/1.2055031

Ho, P., Melius, C. F. Theoretical Study of the Thermochemistry of Molecules in The Si-O-H-C System. Journal of Chemical Physics, 99, 2166-2176 (1995). https://doi.org/10.1021/j100007a056

Hu, G. H., Wang, H. G., Qian, F., Zhang ,Y., Li, J. L. Comprehensive CFD Simulation of Product Yields and Coking Rates for A Floor- and Wall-Fired Naphtha Cracking Furnace. Industrial & Engineering Chemistry Research, 50, 13672-13685 (2011). https://doi.org/10.1021/ie2012642

Kim, E. J., Gill, W. N. Low Pressure Chemical Vapor Deposition of Silicon Dioxide Films by Thermal Decomposition of Tetra-Alkoxysilanes. Journal of the Electrochemical Society, 142, 676-682 (1995). https://doi.org/10.1149/1.2044122

Kleijin, C. R. Computational Modeling of Transport Phenomena and Detailed Chemistry in Chemical Vapor Deposition - A Benchmark Solution. Thin Solid Films, 365, 294-306 (2000). https://doi.org/10.1016/S0040-6090(99)01060-3

Liu, C. J., Chen, Y. Variations of The Microstructure and Mechanical Properties of HP40Nb Hydrogen Reformer Tube with Time at Elevated Temperature. Materials & Design, 32, 2507-2512 (2011). https://doi.org/10.1016/j.matdes.2010.08.031

Olahova, N., Sarris, S. A., Reyniers, M.-F., Marin, G. B., Van Geem, K. M. Coking Tendency of 25Cr-35Ni Alloys: Influence of Temperature, Sulfur Addition, and Cyclic Aging. Industrial & Engineering Chemistry Research, 57, 3138-3148 (2018). https://doi.org/10.1021/acs.iecr.7b04719

Pourmohammad, H., Bahrami, A., Eslami, M., Taghipour, M. Failure Investigation on A Radiant Tube in An Ethylene Cracking Unit. Engineering Failure Analysis, 104, 210-220 (2019). https://doi.org/10.1016/j.engfailanal.2019.05.042

Rahimi, N., Karimzadeh, R., Jazayeri, S. M., Nia, K. D. An empirical investigation of the influence of sulfur additives on the catalytic rate of coke deposition and CO formation in the steam cracking of LPG over Incoloy 600 and stainless steel. Chemical Engineering Journal, 238, 210-218 (2014). https://doi.org/10.1016/j.cej.2013.09.111

Raupp, G. B., Shemansky, F. A., Cale, T. S. Kinetics and Mechanism of Silicon Dioxide Deposition through Thermal Pyrolysis of Tetraethoxysilane. Journal of the Electrochemical Society B, 10, 2422-2431 (1992). https://doi.org/10.1116/1.586034

Reid, R. C., Prausnitz, J. M., Sherwood, T. K. The Properties of Gases and Liquids, Mcgraw-Hill, New York (1977).

Reyniers, G. C., Froment, G. F., Kopinke, F.-D., Zimmermann, G. Coke Formation in the Thermal Cracking of Hydrocarbons. 4. Modeling of Coke Formation in Naphtha Cracking. Industrial & Engineering Chemistry Research, 33, 2584-2590 (1994). https://doi.org/10.1021/ie00035a009

Sadrameli, S. M. Thermal/Catalytic Cracking of Hydrocarbons for the Production of Olefins: State-of-the-art Review I: Thermal Cracking Review. Fuel, 140, 102-115 (2015). https://doi.org/10.1016/j.fuel.2014.09.034

Schietekat, C. M., Sarris, S. A., Reyniers, P. A., Kool, L. B., Peng, W., Lucas, P., van Geem, K. M., Marin, G. B. Catalytic Coating for Reduced Coke Formation in Steam Cracking Reactors. Industrial & Engineering Chemistry Research, 54, 9525-9535 (2015). https://doi.org/10.1021/acs.iecr.5b02263

Song, R., Wu, S. Microstructure Evolution and Residual Life Assessment of Service Exposed Cr35Ni45 Radiant Tube Alloy. Engineering Failure Analysis, 88, 63-72 (2018). https://doi.org/10.1016/j.engfailanal.2018.01.002

Tang, S., Gao, S., Hu, S., Wang, J., Zhu, Q., Chen, Y., Li, X. Inhibition Effect of APCVD Titanium Nitride Coating on Coke Growth during N-hexane Thermal Cracking under Supercritical Conditions. Industrial & Engineering Chemistry Research, 53, 5432-5442 (2014). https://doi.org/10.1021/ie401889p

Tao, W. Q. Numerical heat transfer (2nd ed.). Xi'an Jiaotong University Press, Xi' an (2001).

van Geem, K. M., Heynderickx, G. J., Marin, G. B. Effect of Radial Temperature Profiles on Yields in Steam Cracking. AIChE Journal, 50, 173-183 (2004). https://doi.org/10.1002/aic.10016

van Geem, K. M., Dhuyvetter, I., Prokopiev, S., Reyniers, M.-F. and Marin, G. B., Coke Formation in the Transfer Line Exchanger during Steam Cracking of Hydrocarbons. Industrial & Engineering Chemistry Research, 48, 10343-10358 (2009). https://doi.org/10.1021/ie900124z

Wang, J. D., Reyniers, M.-F., Marin, G. B. Influence of Dimethyl Disulfide on Coke Formation during Steam Cracking of Hydrocarbons. Industrial & Engineering Chemistry Research, 46, 4134-4148 (2007). https://doi.org/10.1021/ie061096u

Wang, J. D., Reyniers, M.-F., van Geem, K. M., Marin, G. B.Influence of Silicon and Silicon/Sulfur-Containing Additives on Coke Formation during Steam Cracking of Hydrocarbons. Industrial & Engineering Chemistry Research, 47, 1468-1482 (2008). https://doi.org/10.1021/ie070970w

Wang, Z. Y., Xu, H., Zhou, J. X., Luan, X. J. Simulation of SiO_2/S Coating Deposition in A Pilot Plant Set-up for Coking Inhibition. Chemical Engineering Research and Design, 91 120 -133 (2013). https://doi.org/10.1016/j.cherd.2012.07.006

Woerde, H. M., Barendregt, S., Humblot, F., Brun, C., Mitigate Coke Formation. Hydrocarbon Processing, 81, 45-50 (2002).

Wu, X. Q., Yang, Y. S., Zhan, Q., Hu, Z. Q. Structure Degradation of 25Cr35Ni Heat-resistant Tube Associated with Surface Coking and Internal Carburization. Journal of Materials Engineering and Performance, 7, 667-672 (1999). https://doi.org/10.1361/105994998770347549

Wu, X. Q., Jing, H. M., Zheng, Y. G., Yao, Z. M., Ke, W. Coking of HP Tubes in Ethylene Steam Cracking Plant and Its Mitigation[J]. British Corrosion Journal, 36, 121-126 (2001). https://doi.org/10.1179/000705901101501541

Zhou, J. X., Xu, H., Liu, J. L., Qi, X. G., Zhang, L., Jiang, Z. M. Study of Anti-coking Property of SiO_2/S Composite Coatings Deposited by Atmospheric Pressure Chemical Vapor Deposition. Materials Letters, 61, 5087-5090 (2007). https://doi.org/10.1016/j.matlet.2007.04.048

Zhou, J. X., Xu, H., Ma, Q. L., Zhang, L., Dai ,Y. L., Peng, B. Mechanical and Thermal Properties of SiO_2/S Composite coating Prepared by APCVD. Materials Science and Engineering A Structural, 491, 147-153 (2008). https://doi.org/10.1016/j.msea.2008.01.092

Zhou, J. X., Wang, Z. Y., Luan , X. J., Xu, H. Anti-coking Property of the SiO_2/S coating During Light Naphtha Steam Cracking in A Pilot Plant Setup. Journal of Analytical and Applied Pyrolysis, 90, 7-12 (2011). https://doi.org/10.1016/j.jaap.2010.09.011